

promoting access to White Rose research papers



Universities of Leeds, Sheffield and York
<http://eprints.whiterose.ac.uk/>

This is an author produced version of a paper published in **Journal of Food Engineering**

White Rose Research Online URL for this paper:
<http://eprints.whiterose.ac.uk/3379/>

Published paper

Lewis R, Yoxall A, Canty LA, Romo ER (2007) *Development of engineering design tools to help reduce apple bruising*, Journal of Food Engineering, Volume 83 (3), 356 – 365.

24 **1 INTRODUCTION**

25 The journey of an apple from the orchard to the supermarket is extremely complex and
26 includes a number of processes such as packaging, sorting, storage and transportation. During
27 these processes the apples have to be treated carefully to maintain quality and avoid losses
28 due to damage. The major contributing factor to such losses is bruising (Garcia et al., 1995;
29 O'Loughlin, 1964). This is defined as damage to, and discolouration of apple flesh, usually
30 with no breach of the skin (Labavitch et al., 1998). The discolouration occurs if damage to
31 the apple causes membranes of the individual cells that make up apple flesh to be breached.
32 This allows enzymes from different parts of the cells to mix initiating a reaction that produces
33 the brown colouration, which is associated with bruising. Recent anecdotal evidence from
34 apple distributors has shown that the wastage figure due to bruising could be 50% or higher.
35 This represents a large cost, not only borne by various parties involved in the journey of the
36 apple from orchard to supermarket, but also by the supermarket, as a significant number of
37 apples are damaged while being put out on display.

38 During its journey to the supermarket an apple may experience a number of different types of
39 loading that may lead to damage and bruising, the two main types being static and dynamic.
40 The dynamic loads may be due to single impacts, which may occur during picking or sorting
41 as the apples are dropped into storage bins, or vibration, which may occur during
42 transportation.

43 In this work the focus was on dynamic loading due to single impacts as this appeared to be
44 the most prevalent. The situations where this may occur are highlighted in Table 1, along
45 with the drop heights and the materials the apples may impact against.

46 Extensive studies of apple bruising due to dynamic impacts have been carried out previously
47 using a variety of techniques, such as drop and pendulum tests and with spring loaded devices

48 to propel an apple against a counterface (Pang et al., 1994; Ragni, 2001; Bollen et al., 2002;
49 Holt, 1977). The data coming from this work, however, is relatively limited in nature and
50 most is in a form that would not be useful to apple distributors or sellers. Pang et al. (1994)
51 have produced the most useful contribution. Their work on dynamic impacts against a variety
52 of counterface materials using a pendulum device produced a series of bruising thresholds.
53 These, however, were based on apple accelerations, which would be harder to determine than
54 drop height for example, which limits their application.

55 The main aim of this work was to develop a numerical design tool for assessing drops
56 typically experienced by apples in harvesting and sorting equipment to reduce the likelihood
57 of apple bruising occurring.

58 Apple drop testing was also carried out against a number of different materials typical of
59 those used in packing, harvesting and storage media to provide easy to interpret results that
60 can be compared with industry thresholds for apple bruises and to provide data to validate the
61 numerical models. Analytical calculations were also used to provide further comparison.

62

63 **2 BACKGROUND**

64 **2.1 Experimental Studies of Dynamic Apple Loading**

65 A number of different testing methods have been used to study dynamic impacts of apples, as
66 mentioned in the introduction. These include simple drop tests (Pang et al., 1994); pendulum
67 tests, in which it is easier to control the impact point as the apple is held (Ragni, 2001; Bollen
68 et al., 2002); tests where a mass is dropped onto a stationary apple (Garcia et al., 1995) and
69 tests using a spring loaded device to propel an apple against a counterface (Holt, 1977).

70 The tests were carried out to try and establish bruise thresholds, either in terms of velocity
71 change at impact or impact energy (which are hard to ascertain); to compare the bruise

72 susceptibility of different apple types and establish the effects of parameters such as
73 irrigation, humidity and time of harvest.

74 Work carried out to study how impact energy affected bruise volume showed that volume
75 was approximately proportional to energy (Holt, 1977). This was for one counterface material
76 and there was no indication of how this may vary with different materials.

77 In general, while giving large amount of useful data on how particular types of apple react to
78 different types of loading under a variety of environmental conditions, the results from these
79 studies of bruising due to impact are very difficult to interpret and compare, and are more
80 importantly do not help apple distributors or sellers in reducing losses due to bruising. Only a
81 small amount of work has been carried out to study impacts against different materials and
82 there has certainly been no attempt to model the impact behaviour to develop a tool for
83 sorting equipment or packaging design.

84

85 **2.2 Apple Finite Element Analysis**

86 Numerical Finite Element (FE) techniques have been used previously to investigate modes of
87 vibration in apples (Lu & Abbott, 1996)) and to study transient responses of apples to
88 impulse excitations to determine factors influencing sonic measurements (Lu & Abbott,
89 1997). Both these analyses were used to ascertain apple firmness, which is a good indication
90 of how ripe an apple is.

91 In the initial study different properties were assigned to each region of the apple (skin, flesh
92 and core), as shown in Table 2. The magnitude of Young's modulus and Poisson's ratio used
93 was found to significantly affect the natural frequencies of vibration. In the second FE study,
94 isotropic elastic properties (of the flesh) were assumed. It was not clear, how the different
95 modelling approaches affected the results as little validation was carried out on either. It

96 could probably be assumed that using different properties for different regions would be a
97 more accurate approach. In both studies a simplified shape was assumed for an apple.

98 FE has also recently been used with some success to investigate contact areas and stresses in
99 static apple contacts (Lewis et al., 2006). In this work, as well as the present study, an actual
100 apple form was generated using laser scanning. This was thought to be important as area and
101 stress will be extremely sensitive to contact geometry.

102

103 **3 EXPERIMENTAL DROP TESTING**

104 The aim of the experimental work was to gain an improved understanding of apple bruise
105 formation due to impacts against a variety of counterface materials and to provide the results
106 in a user friendly form. The results were also to be used to validate analytical and numerical
107 calculations detailed in subsequent sections. A drop testing technique was used, as it was
108 thought to be the most realistic simulation of what would actually happen to the apple,
109 although it was difficult to control the impact point.

110

111 **3.1 Test Apparatus**

112 The drop testing apparatus was relatively simple (see Figure 1). It comprised of a table, the
113 top of which was either the material under examination or the material mounted on a stiffer
114 surface (rubber and cardboard samples were mounted on a steel and perspex counterface
115 respectively to simulate the rubber of a conveyor or a cardboard box on a stiff surface) and a
116 height gauge. In some tests a high speed camera was used to film the contact to determine the
117 impact velocity and rebound distance needed to calculate energy absorbed during the impact.
118 This was set-up to be in line with the impact zone (see Figure 1).

119

120 **3.2 Specimens**

121 ‘Golden Delicious’ apples were used for the tests. This variety was chosen due to its pale
122 skin, which means any discolouration from bruising is more evident. The apples used were on
123 their way to the supermarket, having been in cold storage. Sugar content and firmness tests
124 were carried out on the apples prior to testing to ensure that apples with consistent properties
125 were used. A spherometer was used to measure the radii of curvature of the apples at the *stem*
126 *shoulder*, *cheek* and *calyx shoulder* regions (see Figure 2a) to enable relationships between
127 bruising and location of impact on the apples to be determined and to provide input data for
128 Hertz predictions of the contact area and stress to be calculated. The results of the
129 measurements are shown in Figure 2b. As would be expected *cheek* radii were higher than
130 those of the *calyx* and *stem shoulders*.

131 The properties shown in Table 2 for ‘Golden Delicious’ apples were used throughout this
132 work. They were taken from tests carried out by Abbott & Lu (1996) and Mohsenin (1970).
133 This work indicated that the elastic properties of the apple flesh varied according to load
134 orientation and position in the apple (data in Table 2 has been averaged). Failure stresses
135 were also determined for the flesh and these also varied with position in the apple. Typical
136 values were around 0.40-0.51MPa, although, as with all properties, these varied with the
137 relative ripeness of the apples. The greatest failure stresses were found for *medium* ripe
138 apples (levels of relative *ripeness* were based on harvest time and appearance).

139 A number of different materials were used in the drop tests as impact surfaces. These were
140 chosen based on the data collected in Table 2. Their properties are shown in Table 3. The
141 cardboard was Type 150B corrugated board, as shown in Figure 3. Dimensions for the
142 cardboard are shown in Table 4. Data for mechanical properties of such cardboard are quite
143 limited. The values shown in Table 3 were taken from work to determine the elastic constants
144 of corrugated board panels.

145 3.3 Procedure

146 Apples were dropped from heights ranging from 0.1 – 1.2m (to cover the range of possible
 147 heights identified in Table 1) onto perspex, steel, rubber (on steel), cardboard (on perspex)
 148 and wood as well as a half apple to simulate an apple-to-apple contact. Tests were repeated
 149 for each height at least three times to ascertain the spread of results.

150 The aim was to achieve apple impact in the *cheek* region, however, initial testing indicated
 151 that it was quite difficult to control the impact position. It was possible, though, using the
 152 measurements taken of each apple pre-test, to tie up bruise volumes with radius of the apple
 153 at the impact point. A number of tests were therefore carried out to assess how the bruise
 154 areas and volumes varied with radius at contact and region of contact (using a perspex
 155 counterface).

156 Apples were left for 24 hours after dropping for the bruises to develop fully. The areas, A ,
 157 were then determined by measuring the widths ($2a$ and $2b$, as shown in Figure 4) and
 158 assuming they were elliptical:

$$159 \quad A = \pi ab \quad (1)$$

160 Bruise volumes were calculated using the *elliptical bruise thickness method* (Mohsenin,
 161 1970). This calculation method has been compared with a range of others and found to give
 162 the most accurate results (Bollen et al., 1999). Bruise volume, V is given by:

$$163 \quad V = \frac{\pi(d_b - d_t)}{24} (12ab + 4(d_b - d_t)^2) \quad (2)$$

164 The parameters used are defined in Figure 4.

165 High speed video footage was taken of an apple-to-steel, apple-to-perspex and apple-to-apple
 166 contact at heights of 0.1, 0.3 and 0.6m. The filming and analysis process was extremely time
 167 consuming so tests were not carried out with all materials.

168 The captured film was processed and software was used to find the co-ordinates of the apples
169 as they fell by placing circles around them in each frame, as illustrated in Figure 5.

170 Calculations could then be carried out to determine the impact energy, e_{impact} , which is equal
171 to the difference between the energy the apple has before and after the impact:

172 Energy before, $e_{before} = mgh_{drop}$ (3)

173 Energy after, $e_{after} = mgh_{after} + \frac{1}{2}mv_{after}^2$ (4)

174 Impact energy, $e_{impact} = e_{before} - e_{after}$ (5)

175 where m is the apple mass, v is the apple velocity, h_{drop} is the drop height and h_{after} the height
176 after impact.

177

178 3.4 Results

179 Results of tests carried out to see how the location of the impact point on the apple would
180 affect bruise volume are shown in Figure 6. Results have been selected so that the *cheek*, *stem*
181 *shoulder* and *calix shoulder* radii were similar at each drop height to allow the results to be
182 considered independent of the geometry (the radii for the *cheek*, *stem shoulder* and *calix*
183 *shoulder* were: ~40mm, ~30mm and ~35mm respectively). As can be seen the largest bruises
184 are seen on the *cheeks*. These typically have larger radii, so there is clearly a relationship
185 between radii and bruise volume. A plot of radius against bruise area against bruise volume is
186 shown in Figure 7. This shows that bruise area and volume clearly increase with increasing
187 radius.

188 Average apple bruise areas and volumes (calculated using Equations 1 and 2) after impacts
189 against a variety of counterface materials are shown in Figures 8 and 9. Spread in bruise size

190 over the three specimens used at each test condition was a maximum of $\pm 50\text{mm}^2$. The
191 smallest bruises were seen when using cardboard and wood and the largest with steel and
192 rubber on steel. In the apple-to-apple tests the stationary apples had larger bruises than the
193 dropped apple.

194 On Figure 8, showing bruise areas, the industry threshold for bruises (100mm^2) is also plotted
195 as well as possible regimes of damage at the various stages of the apple journey. It can be
196 determined at what drop height this is exceeded for each of the counterface materials, which
197 is very useful information when designing equipment for harvesting and sorting or packaging
198 media.

199 Data in Figure 10 illustrates how bruise volume varies with impact energy. Values
200 determined using the high speed video footage and Equations 3-5. There is an approximately
201 linear relationship between the two, with different gradients for each counterface material.
202 This ties in with observations made by Holt (1977) during tests with 'Jonica' apples, the
203 results of which are also shown in Figure 10.

204

205 **4 DYNAMIC FINITE ELEMENT MODELLING**

206 **4.1 Mesh Construction**

207 In order to use the geometry of an actual apple in the FE modelling, a laser scan was created
208 of a Golden Delicious apple, which was then imported into ANSYS LS-DYNA software to
209 create a mesh. The apple prepared for scanning is shown in Figure 11a. The apple was
210 sprayed white to provide a reflective surface for the laser scanner. The geometry of a real
211 apple is complex and non-symmetrical so the volume was free meshed with tetrahedral
212 elements, as shown in Figure 11b. It was found that a density of 17000 elements was

213 sufficient to accurately represent the apple geometry and also allowed the model to be solved
214 with the resources available.

215 To simplify the modelling, isotropic properties were assumed, as they have been in most
216 previous FE studies of apples (see Section 2.2).

217 A Young's modulus of 4MPa was used, as determined for 'Golden Delicious' flesh in the
218 appropriate region of the apple by Abbot & Lu (1996). The data in Table 2 illustrates shows
219 how the Young's Modulus actually varies between the various parts of an apple. Abbott & Lu
220 (1996) have also shown that the properties of apple flesh vary in different parts of the apple
221 and are different if loading is applied from varying directions.

222 Linear elastic material properties were also assumed, and while this is probably not valid for
223 apple flesh, it is compatible with previous work.

224

225 **4.2 Modelling Procedure**

226 Dynamic analysis was used to simulate a free fall of the meshed apple for drop heights of 0.2
227 to 1.2m onto the impact surface, as illustrated in Figure 12. Impact surfaces were given the
228 properties shown in Table 3. Model runs were carried out for impacts on perspex, wood and
229 cardboard. In order to reduce the calculation time, only the short time frame after impact was
230 analysed. Impact velocities were calculated from the drop heights ($v = \sqrt{2gh}$) and are shown
231 in Table 5.

232

233 **4.3 Results**

234 Figure 13 shows the evolution of the apple during an impact onto perspex from a height of
235 1.2m. The picture on the left is at initial contact with the counterface. During the impact the

236 contact area and stresses increase. Figure 14 shows a snap shot of the point at which the
 237 stresses are at a maximum (at maximum deflection). In order to estimate a *bruise area*, the
 238 area of the contact in each case over 0.5MPa (approximate failure stress of ‘Golden
 239 Delicious’ apple flesh (Abbott & Lu, 1996)) was calculated. Full results are compared with
 240 the experimental and analytical results in the discussion.

241

242 5 ANALYTICAL ANALYSIS

243 Analytical calculations for the impacting apples were based on a scheme using Hertz
 244 equations for contacts (Hertz, 1881). This analysis, although both static and elastic in nature
 245 has been widely applied to impact situations where permanent deformations are produced,
 246 such as the apple contact. The use of the Hertz analysis beyond the limits of its validity has
 247 been justified on the basis that it appears to predict accurately most of the impact parameters
 248 that can be experimentally verified (Goldsmith, 1960).

249 Initially the impact force, P_{\max} , was calculated using analysis derived for an elastic sphere
 250 impacting a rigid plate (Goldsmith, 1960):

$$251 \quad P_{\max} = k_h \delta_{\max}^{1.5} \quad (6)$$

252 where δ_{\max} , is the maximum deflection given by:

$$253 \quad \delta_{\max} = \left(\frac{5}{4} m \frac{v_0^2}{k_h} \right)^{0.4} \quad (7)$$

254 where m is the mass of the sphere, v_0 is the sphere velocity at impact (given by $\sqrt{2gh}$, where
 255 h is the drop height) and k_h is a constant given by:

$$256 \quad k_h = \frac{3}{4} R^{0.5} \frac{E}{(1-\nu^2)} \quad (8)$$

257 where R is the radius of the sphere (the average value of the *cheek* region of the apple was
 258 used) and E and ν are Young's modulus and Poisson's Ratio of the sphere material
 259 respectively. Results of calculations for a range of drop heights are shown in Table 5 (values
 260 of E and ν for apple flesh in Table 2 were used and an apple mass of 0.15kg).

261 Once the force has been calculated it can be used in the following Hertz equations to
 262 determine the elliptical contact area half widths a and b and the maximum contact pressure p_0
 263 (equations are outlined in Williams (1994)).

264 Results of these calculations for an apple impact on perspex are shown in Table 5. Properties
 265 for the apple flesh and counterface materials given in Table 5 were used in the calculations.
 266 Average values from the measurement of apple specimens in the drop testing were used to
 267 determine R_1 (28.8mm) and R_2 (37mm). The contact area does not represent the likely bruise
 268 area. To determine area approximations for the bruises the pressure distributions were plotted
 269 (as shown in Figure 15 for perspex) using the equation given below:

$$270 \quad p = p_0 \left\{ 1 - \left(\frac{x}{a} \right)^2 - \left(\frac{y}{b} \right)^2 \right\}^{1/2} \quad (9)$$

271 A plot is shown for a perspex impact at a range of drop heights for sections along the x axis.
 272 The x and y axis plots were used to determine a and b can be determined from the plots at the
 273 point where the stress is over 0.5MPa, the failure stress of 'Golden Delicious' apple flesh.
 274 Comparison of the results of the calculations with the FE and experimental results are
 275 included in the discussion.

276

277 **6 DISCUSSION**

278 Data has been generated in this work that can be used by designers of apple harvesting,
 279 sorting and packing equipment to reduce the likelihood of apple bruises occurring. Drop

280 heights can be reduced to levels below those that could give a bruise over the industry
281 threshold size (see Figure 8). Although bruise volumes have been calculated throughout the
282 work, it is probably bruise areas that are more important as these are visible and used to
283 define the threshold used. It is also usually how an apple looks that determines whether a
284 consumer will purchase it (Cliff et al., 2002).

285 The work has shown that the radius at the point of impact heavily influences the bruise
286 volume, with larger radii giving larger bruises. This means that if the point of impact is on the
287 *cheek* of an apple, the bruise will be larger than those on the *stem* or *calix shoulders*, which
288 generally have smaller radii.

289 It was clear from the results that using counterface materials with a higher energy absorbing
290 capacity led to smaller apple bruises. The rubber, however, because it was backed with steel
291 still gave relatively large bruises. It was also interesting to see that large bruises occurred due
292 to apple-to-apple contacts. This can occur when apples are tipped, for example, into display
293 stands in supermarkets and if this is done from too high a height problems may occur and
294 lead to apple wastage.

295 It should be noted here that the tests were carried out for a set of apples at one condition. The
296 apples tested had come out of storage and were on their way to a supermarket. At other stages
297 of ripeness they would have had different properties. Previous work has also shown that
298 varying irrigation conditions, humidity and harvest time will affect the mechanical properties
299 of apples and the bruise sizes will vary accordingly (Garcia et al., 1995). Also work has
300 shown that bruise susceptibility changes with apple variety (Pang et al., 1994; Ragni, 2001).
301 In future development of the modelling this will have to be accounted for.

302 Figure 16 shows how the analytical and numerical *bruise* predictions for perspex, wood and
303 cardboard compare with the experimental results. Good correlation is seen for all, even with
304 the simplifications made in modelling the corrugated board.

305 The numerical and analytical modelling illustrates the fact that the bruise area is lower than
306 the actual bruise area. When considering just the area at the failure stress of the apple flesh a
307 better prediction of bruise size is achieved. The relationship between contact area and bruise
308 area has been shown experimentally previously in work on apple-to-apple contacts (Pang et
309 al., 1992; Studman et al., 1997) where bruise areas were up to 25% lower than the contact
310 area. The analytical results in the present study illustrated in Figure 16 show a difference of a
311 similar order of magnitude (where unmodified Hertz is the contact area and the modified
312 Hertz is the bruise area).

313 The numerical model clearly shows great promise, and if developed further to improve the
314 structure of the apple, and combined with the static approach detailed previously (Lewis et
315 al., 2006), could create a comprehensive tool for assessing apple packaging. The results could
316 also be used as part of educational tools for those working in the industries dealing with
317 apples and other produce, to help reduce the likelihood of damage occurring.

318

319 **7 CONCLUSIONS**

320 Apple bruise areas and volumes resulting from dynamic impacts vary with surface radii of the
321 apple at the point of impact. The larger the radii the larger the area and volume of the bruise
322 formed. Therefore *cheek* impacts will give larger bruises than *stem* or *calix* shoulder impacts
323 as this region tends to have a higher radius.

324 Experimental data has been generated for bruise area and volumes for impacts against a
325 number of different counterface materials and for a range of drop heights. This has shown

326 that bruise volume is approximately proportional to drop height. Rigid counterfaces gave
327 higher bruise areas than softer more energy absorbing materials. Figure 17 shows the
328 relationship between the Young's Modulus of the counterface materials and the bruise
329 volume at a drop height of 1m (from Figure 9). The trend is clearly for bruise volume to grow
330 with increasing Young's modulus. The only anomaly is rubber, but the value plotted is that
331 for rubber alone and the rubber was actually mounted on a steel base plate which would
332 increase the overall stiffness. The data has been compared with industry thresholds for bruise
333 sizes and indicates maximum drops heights that should be allowed to give bruises below
334 these.

335 Analytical and numerical tools have been developed to predict bruise sizes for a given drop
336 height against a given counterface material. The numerical model particularly shows
337 reasonable correlation with experimental results and if developed further and combined with
338 previously developed static models will provide a comprehensive design tool for apple
339 harvesting and transportation equipment and packaging media. Average differences ranged
340 between 7% for Perspex to 18% for wood and 26 % for cardboard. It was in modelling the
341 cardboards as a homogeneous material, however, that the largest simplification was made so
342 this error is perhaps not surprising.

343

344 **8 REFERENCES**

345 Abbott, J.A. & Lu, R. (1996). Anisotropic mechanical properties of apples. *Transactions of*
346 *the ASAE*, 39, 1451-1459.

347 Bollen, A.F., Cox, N.R., Dela Rue, B.T. & Painter, D.J. (2002). A descriptor for damage
348 susceptibility of a population of produce. *Journal of Agricultural Engineering Research*, 78,
349 391-395.

- 350 Bollen A.F., Nguyen H.X. & Dela Rue B.T. (1999). Comparison of methods for estimating
351 the bruise volume of apples. *Journal of Agricultural Engineering Research*, 74, 325-330.
- 352 Cliff M., Sanford K., Wismer W. & Hampson C. (2002). Use of digital images for evaluation
353 of factors responsible for visual preference of apples by consumers. *Hortscience*, 37, 1127-
354 1131.
- 355 Garcia, J.L., Ruiz-Altisent M. & Barreiro, P. (1995). Factors influencing mechanical
356 properties and bruise susceptibility of apples and pears. *Journal of Agricultural Engineering
357 Research*, 61, 11-18.
- 358 Goldsmith W. (1960). *Impact: The theory and physical behaviour of colliding solids*. Edward
359 Arnold Ltd, London.
- 360 Hertz H. (1881). Über die Berührung fester elastischer Körper. *Journal reine angew Mat.*, 92,
361 155.
- 362 Holt, J.E. & Schoorl, D. (1977). Bruising and energy dissipation in apples. *Journal of
363 Textures Studies*, 7, 421-432.
- 364 Labavitch, J.M., Greve, L.C. & Mitcham, E. (1998). Fruit bruising: it's more than skin deep.
365 *Perishables Handling Quarterly*, 95, 7-9.
- 366 Lewis, R., Yoxall, A., Marshall, M.B., Canty, L.A. (2006). Characterising pressure in apple
367 contacts. submitted to *Wear*.
- 368 Lu, R. & Abbott, J.A. (1996). Finite element analysis of modes of vibration in apples.
369 *Journal of Texture Studies*, 27, 265-286.
- 370 Lu, R. & Abbott, J.A. (1997). Finite element modelling of transient responses of apples to
371 impulse excitation. *Transactions of the ASAE*, 40, 395-1409.
- 372 Lu, T.J. & Zhu, G. (2001). The elastic constants of corrugated board panels. *Journal of
373 Composite Materials*, 35(20), 1868-1870.
- 374 Mohsenin, N.N. (1970). *Physical Properties of Plant and Animal Materials*. Vol. 1, Gordon
375 and Breach Publishers, New York.
- 376 O'Loughlin, JB. (1964). The bruising of fruit during transport and storage. In *Proceedings of
377 the Fourth Australian Fruit and Vegetable Storage Conference*, 1-13.
- 378 Pang, D.W., Studman, C.J. & Banks, N.H. (1994). Apple bruising thresholds for an
379 instrumented sphere. *Transactions of the ASAE*, 37, 893-897.

380 Ragni, L. & Berardinelli, A. (2001). Mechanical behaviour of apples and damage during
381 sorting and packaging. *Journal of Agricultural Engineering Research*, 78, 273-279.

382 Williams, J.A., (1994). *Engineering Tribology*, Oxford University Press, Oxford.

383 Pang, W., Studman, C.J., Ward, G.T. (1992). Bruising damage in apple-to-apple impact.
384 *Journal of Agricultural Engineering Research*, 52, 229-240.

385 Studman, C.J., Brown, G.K., Timm, E.J., Schulte, N.L., Vreede, M.J. (1997). Bruising on
386 blush and non-blush sides in apple-to-apple impacts. *Transactions of the ASAE*, 40(6), 1655-
387 1663.

388

389 **Figure Captions**

- 390 Figure 1 Drop Test Apparatus and Camera Set-up
- 391 Figure 2 (a) Regions where Radii of Curvature were Measured; (b) Values of Radii
- 392 Figure 3 Corrugated Card used in Impact Testing
- 393 Figure 4 Elliptical *Bruise Thickness* Method for Bruise Determination (Mohsenin,
394 1970)
- 395 Figure 5 Circles Placed around Apples in Film Data Analysis
- 396 Figure 6 Bruise Volumes for Apples Dropped onto the *Cheek* (~40mm radius), *Calix*
397 *Shoulder* (~35mm radius) and *Stem Shoulder* (~30mm radius) from various
398 Heights on to Perspex (radii were similar for each apple impact point for each
399 of the tests)
- 400 Figure 7 Bruise Area and Volume against Radius of Apple at Impact Point
- 401 Figure 8 Average Bruise Areas for Apple Impacts against Different Materials at
402 Varying Drop Heights
- 403 Figure 9 Bruise Volumes for Apple Impacts against Different Materials at varying Drop
404 Heights
- 405 Figure 10 Bruise Volume against Impact Energy for Different Impact Surfaces
- 406 Figure 11 The Apple (a) Before Laser Scanning and (b) Represented in Ansys
- 407 Figure 12 Finite Element Model of Apple and Impact Surface
- 408 Figure 13 FE Apple Impact against Perspex from a Drop Height of 1.2m at Point of
409 Maximum Deflection
- 410 Figure 14 Stresses in a Node at the Centre of the Contact in Figure 18
- 411 Figure 15 Stress Distributions for Drop Heights from 0.2m to 1.2m onto Perspex
- 412 Figure 16 Comparison of Experimental, Analytical and Numerical Bruise Areas for
413 Apple Impacts against Perspex, Wood and Cardboard
- 414 Figure 17 Bruise Volume at a 1m Drop Height (from Figure 9) against Young's Modulus
415 of the Counterface Material

416

417 **Table Captions**

- 418 Table 1 Potential Dynamic Apple Loading Situations and Associated Drop Heights
- 419 Table 2 Young's Modulus, Poisson's Ratio and Failure Stress for Different Parts of a
420 Golden Delicious Apple (Abbott & Lu, 1996; Mohsenin, 1970)
- 421 Table 3 Impact Surface Material Properties
- 422 Table 4 Geometrical Characteristics and Bulk Density of Type 150B Corrugated
423 Board
- 424 Table 5 Results of Analytical Apple Impact Calculations

Figure 1

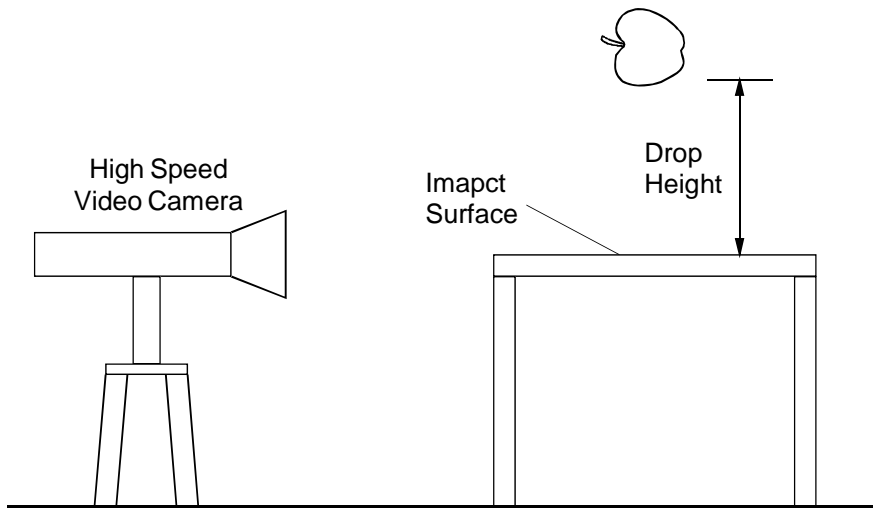


Figure 2

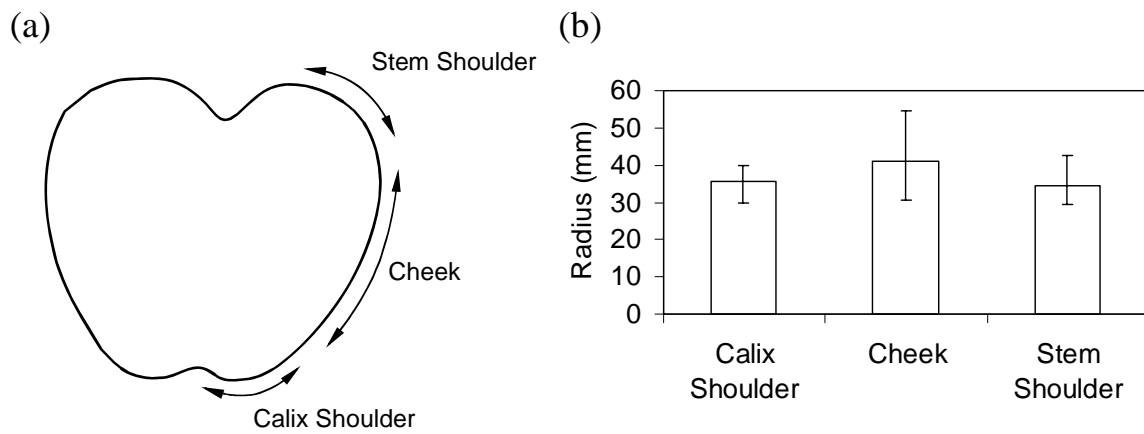


Figure 3

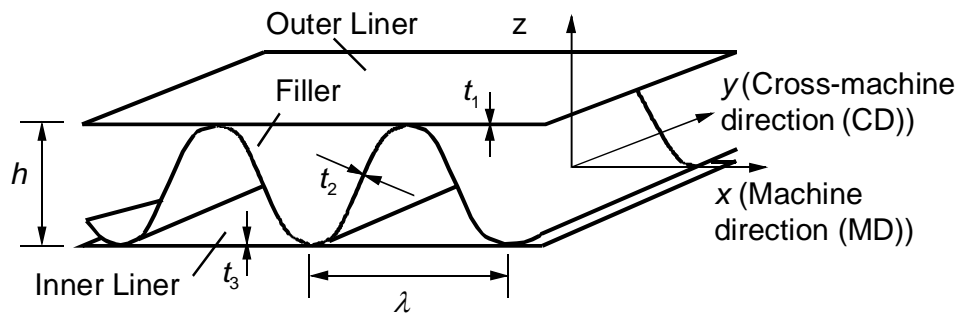


Figure 4

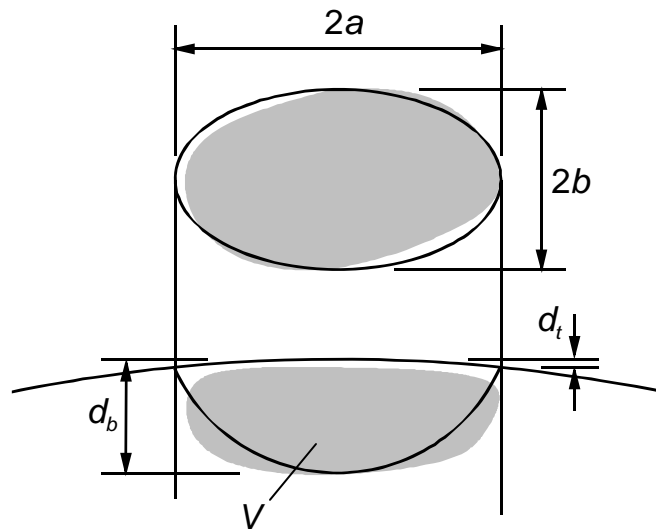


Figure 5

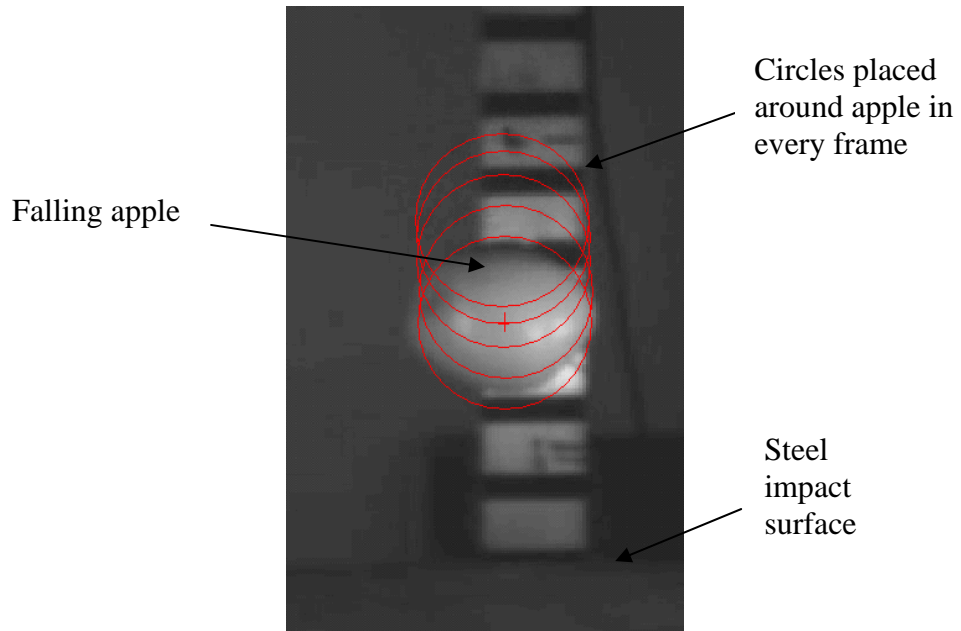


Figure 6

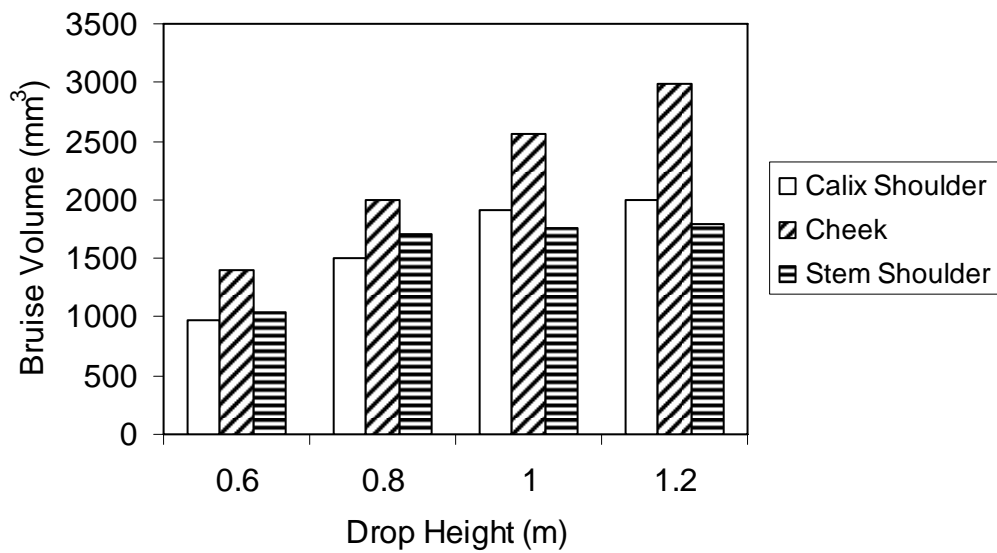


Figure 7

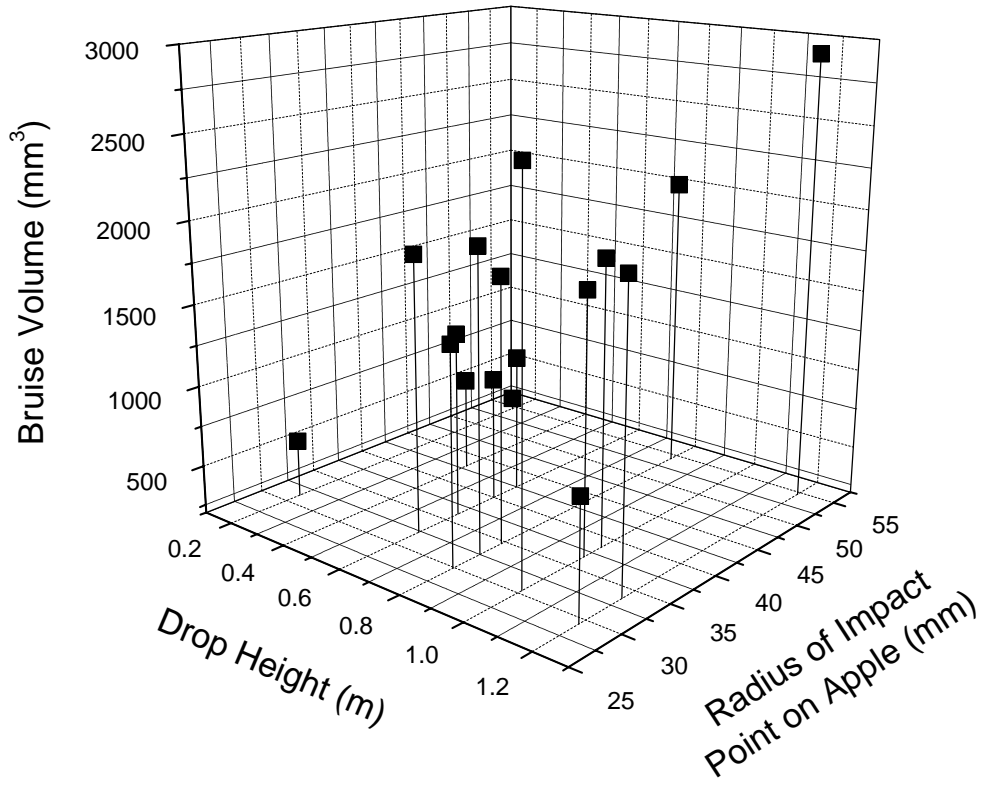


Figure 8

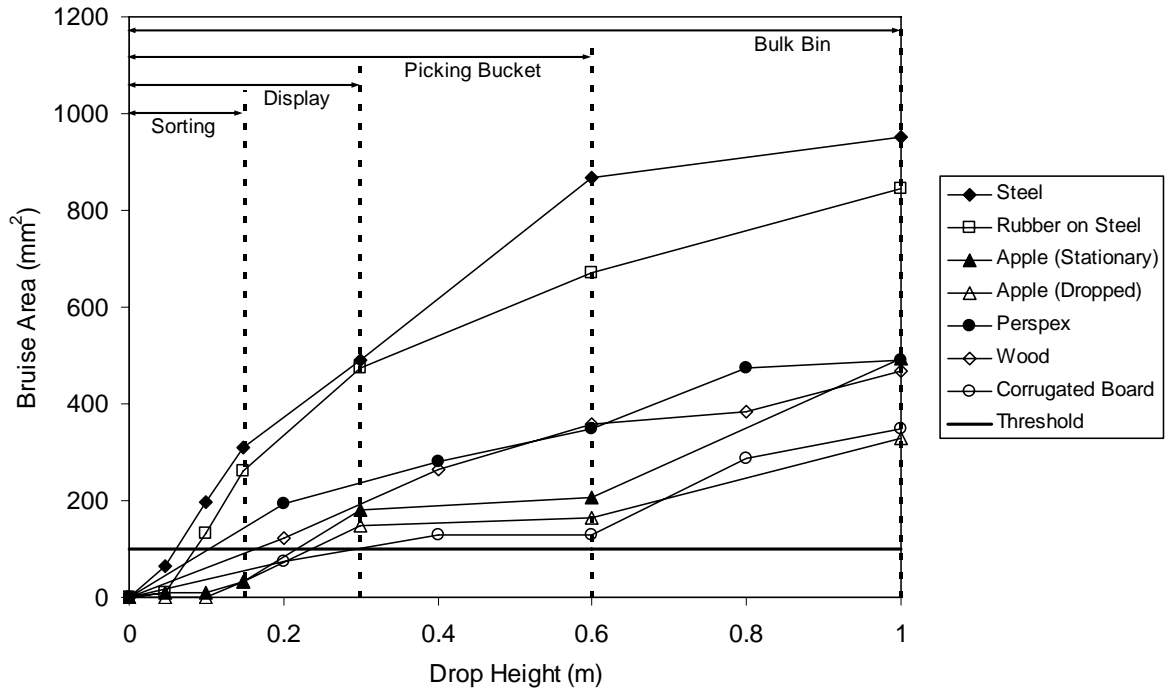


Figure 9

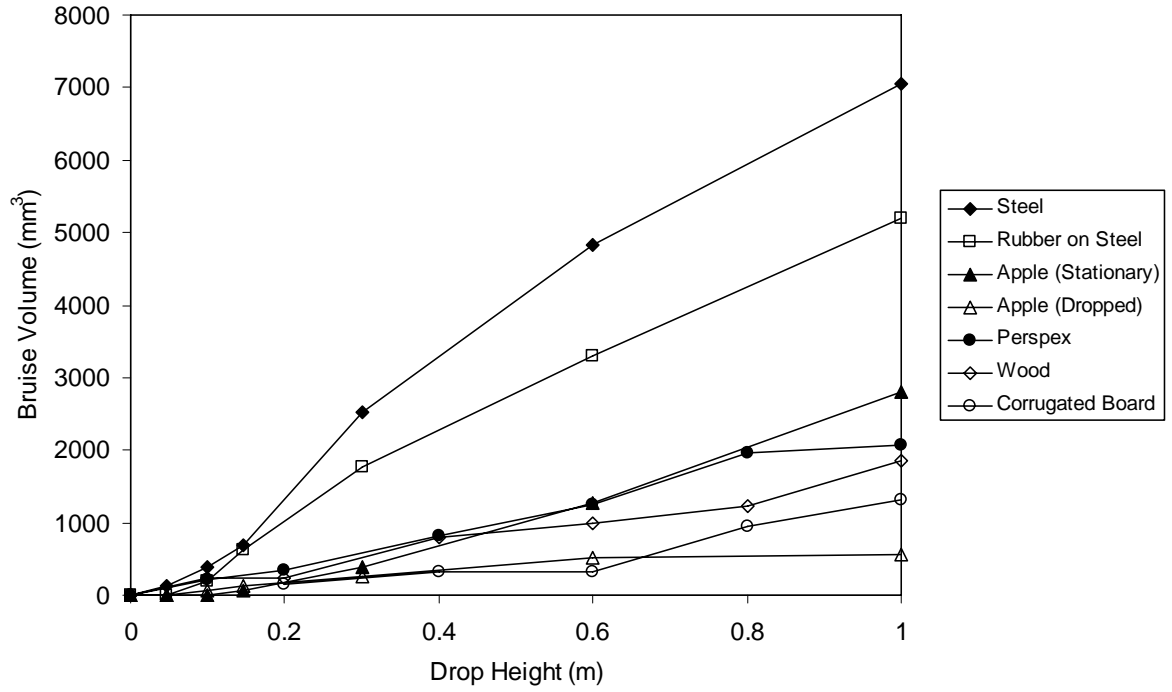


Figure 10

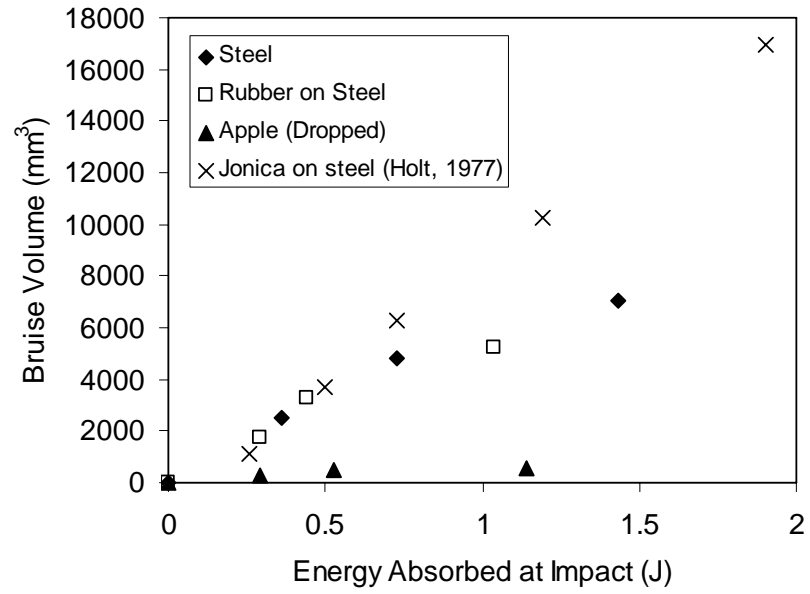


Figure 11

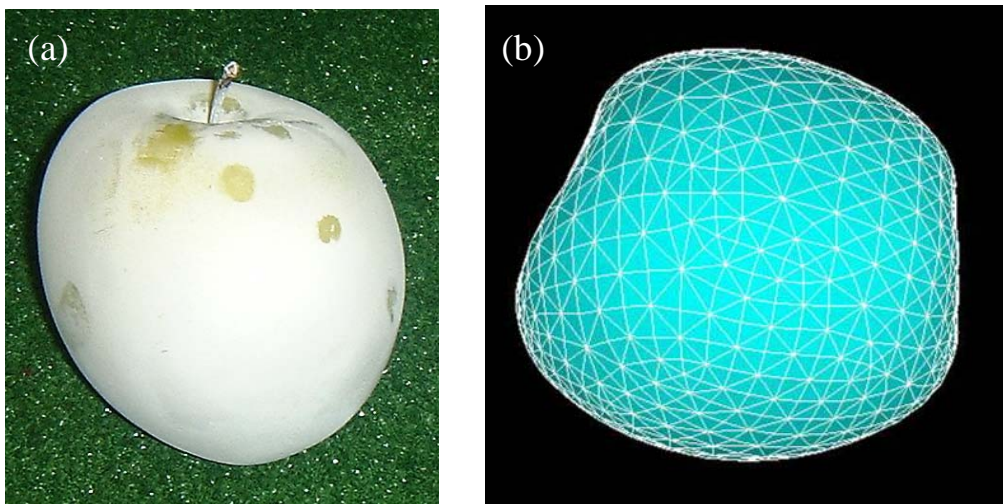


Figure 12

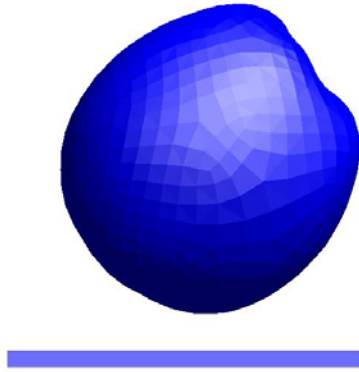


Figure 13

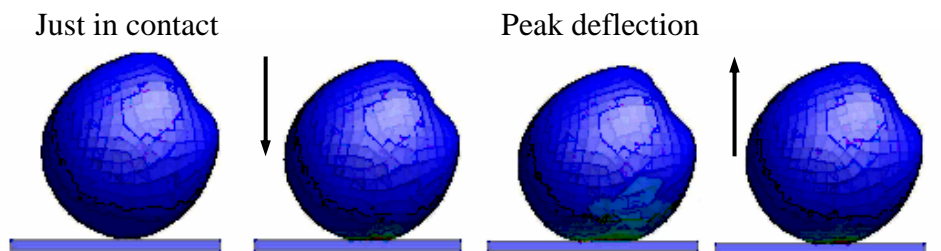


Figure 14

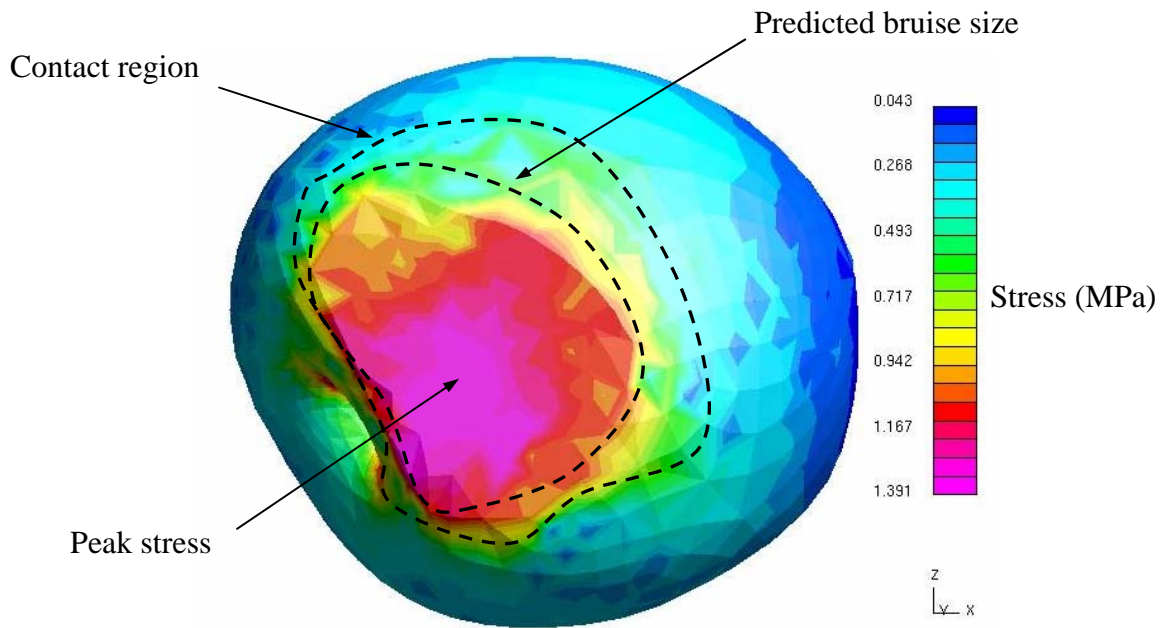


Figure 15

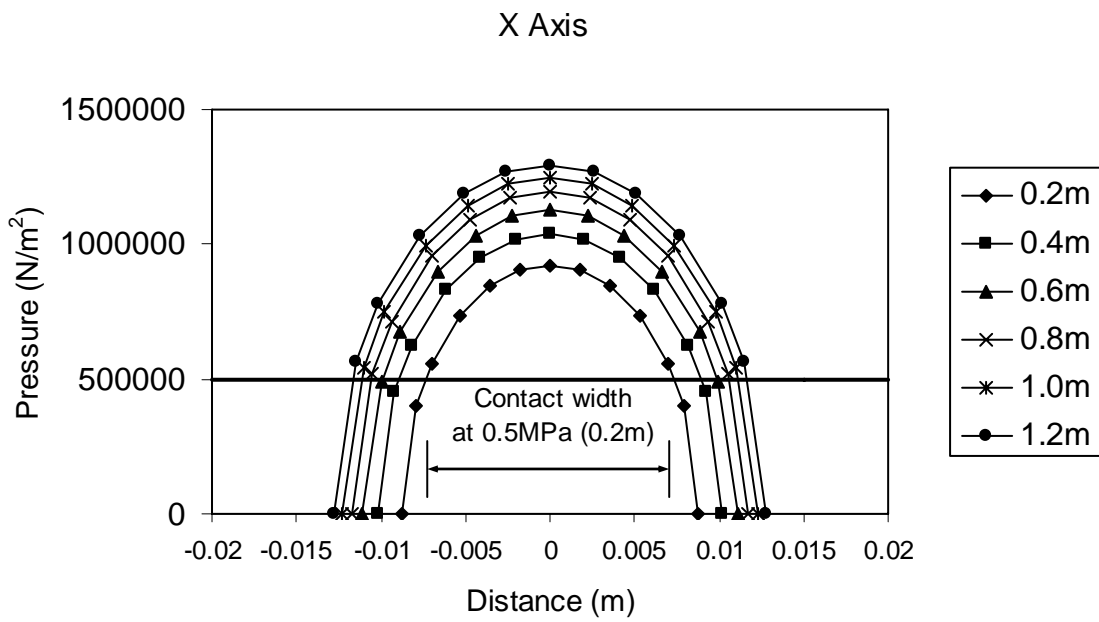


Figure 16

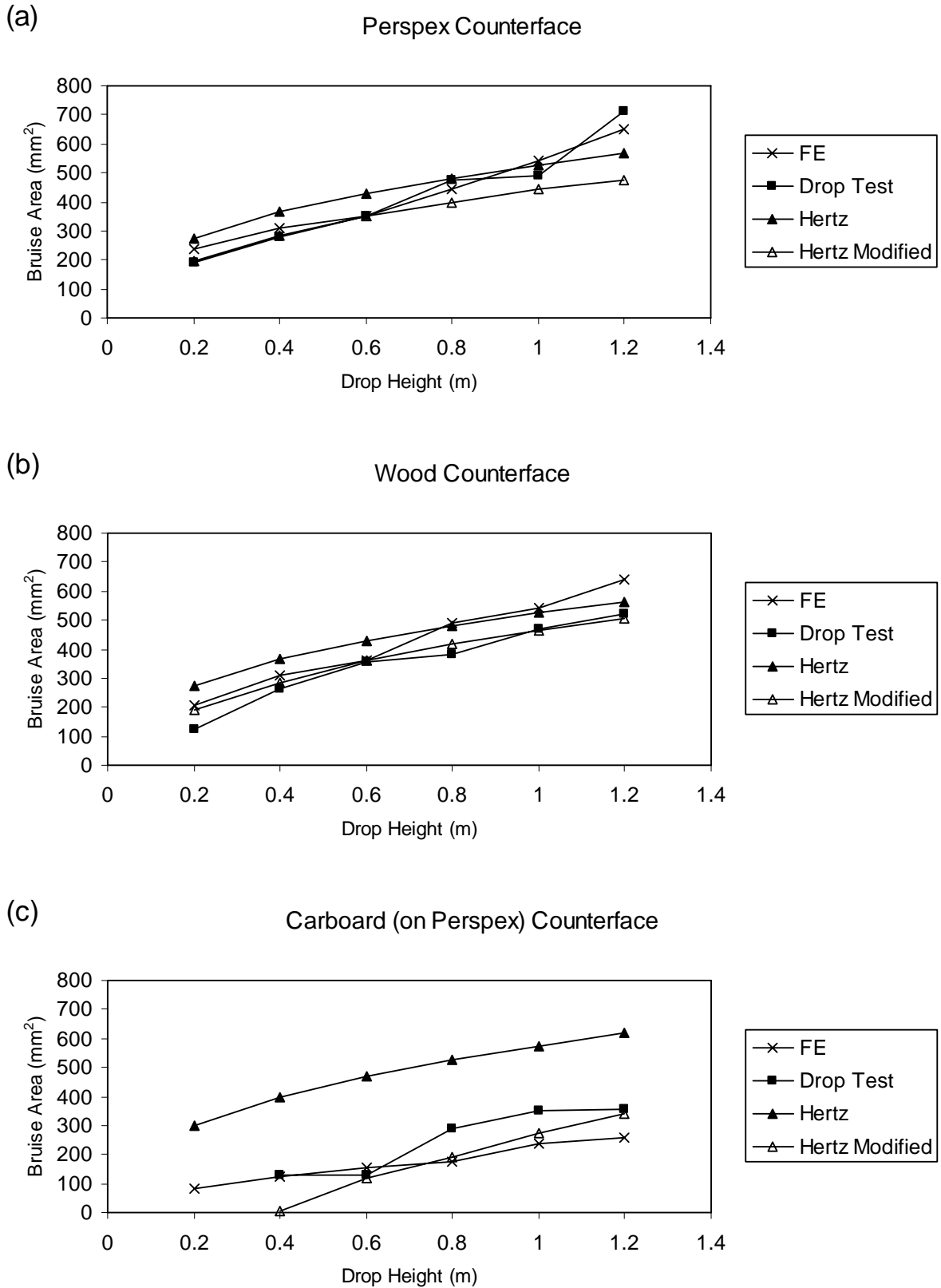


Figure 17

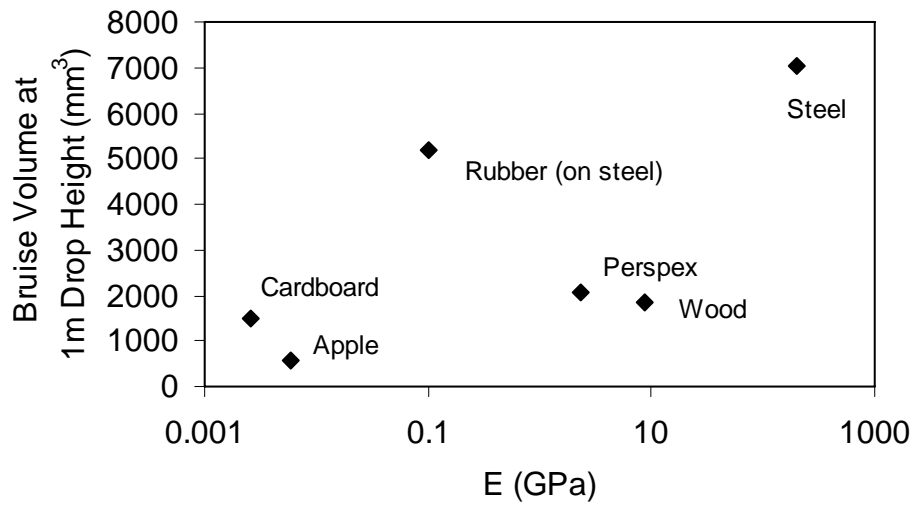


Table 1

Point in Journey	Process Stage	Potential Drop Height	Impact Material
Orchard	Picking Bucket	0.6m	Perspex Wood Apple
	Bulk Bin	0.6-1m	
Packing House	Repack	0.05-0.15m	Perspex Wood Cardboard Apple
Distributor	Sorting (conveyors etc.)	0.05-0.15m	Steel Rubber on Steel
Retailer	Putting on Display	0.05-0.3m	Cardboard Apple

Table 2

Region of Apple	Skin	Flesh	Core
Young's Modulus (MPa)	20	4	8
Failure Stress (MPa)	-	0.40-0.51	-
Poisson's Ratio	0.3	0.3	0.3

Table 3

Material	Thickness (mm)	Elastic Modulus, E (GPa)	Poisson's Ratio, ν
Perspex	5	2.35	0.38
Steel	5	200	0.3
Rubber	3	0.1	0.5
Wood (Pine)	8	8.89	0.341
Cardboard	3	0.0026 (E_r)	0.01

Table 4

Parameter	Value
h (mm)	2.9
λ (mm)	6.5
t_1	0.25
t_2	0.25
t_3	0.25
Bulk Density (kg/m ³)	194.8

Table 5

Drop Height (m)	Velocity at Impact (m/s)	δ_{\max} (m)	P_{\max} (N)	R' (mm)	k	E	E^* (N/m ²)	a (mm)	b (mm)	Area (mm ²)	Mod. Area (mm ²)
0.2	1.98	0.00416	169.9	16.2	0.882	1.46	4.39×10^{-6}	9.80	9.98	276.03	195.51
0.4	2.80	0.00548	257.6	16.2	0.882	1.46	4.39×10^{-6}	10.11	11.47	364.23	284.49
0.6	3.43	0.00645	328.5	16.2	0.882	1.46	4.39×10^{-6}	10.96	12.44	428.36	350.42
0.8	3.96	0.00724	390.4	16.2	0.882	1.46	4.39×10^{-6}	11.61	13.17	480.60	395.98
1	4.43	0.00791	446.3	16.2	0.882	1.46	4.39×10^{-6}	12.14	13.77	525.47	441.37
1.2	4.85	0.00851	497.9	16.2	0.882	1.46	4.39×10^{-6}	12.59	14.28	565.22	476.15